A&A manuscript no.
(will be inserted by hand later)

Your thesaurus codes are:
11 (11.09.1; 11.09.5; 11.19.2; 13.09.1)

ASTRONOMY
AND
ASTROPHYSICS
31.10.1996

Analysis of the ISOPHOT FIR Maps of M 51 and M 101 *

H. Hippelein[1], D. Lemke[1], M. Haas[1], C.M. Telesco[3], R.J. Tuffs[2], H.J. Völk[2], C. Xu[2], U. Klaas[4], and U. Kinkel[4]

[1] Max–Planck–Institut für Astronomie, Königstuhl 17, D-69117 Heidelberg, Germany
[2] Max–Planck–Institut für Kernphysik, Saupfercheckweg, D-69117 Heidelberg, Germany
[3] Department of Astronomy, University of Florida, Gainesville, FL 32611, USA
[4] Max–Planck–Institut für Astronomie, Königstuhl 17, D-69117 Heidelberg, Germany
at present ISO Ground Observatory, Villafranca, Spain

Received ??; accepted ??

Abstract. The far-IR ISOPHOT maps of the spiral galaxies M 51 and M 101 at 60, 100, and at 175 μm are analysed. For all areas in these galaxies the spectral energy distributions can be fitted with a single-temperature emission curve. Colours and dust temperatures were estimated for interesting sub-fields. The temperatures vary between 33 K for H II regions, and 28 K for the disk, arm and interarm regimes.

Key words: galaxies – star formation – dust

1. Introduction

M 101 and M 51 are nearby archetypes of galaxies with an open spiral structure that is rich with young stars and dark filaments. The nearly face-on orientation of these galaxies makes them especially useful for studying the relationship between far-IR emission and other galactic components such as molecular material and non-thermal radio emission. In Hippelein et al. (1996, Letter 1), we presented maps of M 101 and M 51 obtained with ISOPHOT at 60, 100 and 175 μm. In the present Letter we explore some of the more obvious implications of these maps. In particular, we compare their far-IR morphology with those at other wavelengths, and we examine the spatial distribution of the temperature of the far-IR emitting dust.

Send offprint requests to: H. Hippelein

* ISO is an ESA project with instruments funded by ESA Member States (especially the PI countries: France, Germany, the Netherlands and the United Kingdom) and with the participation of ISAS and NASA.

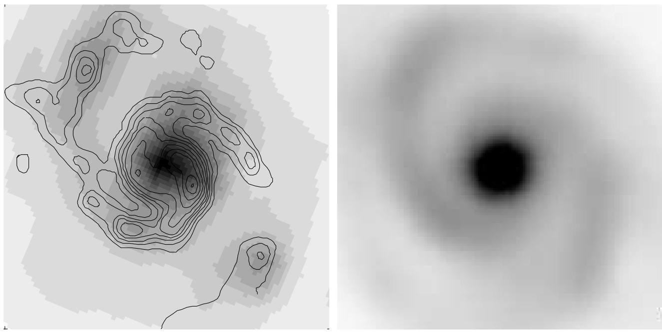

Fig. 1. Left: CO contour map for the central $5' \times 5'$area of of M 51 by Garcia-Burillo et al (1993), overlaid on the ISOPHOT 60 μm map. Right: Smoothed red image, in the same scale.

2. Results

For the morphology discussion we will only use the 60 μm images which have the highest spatial resolution. Figure 1 shows the central $5'$ area of the 60 μm ISO map of M 51 (left), overlaid with a contour map of the CO integrated intensity in the ^{12}CO(2–1) line (Garcia-Burillo et al. 1993), and an R band image taken with the 70 cm telescope at the MPI für Astronomie in Heidelberg and smoothed to an angular resolution of $45''$(right),

The dominant features in the 60 μm image are the two lobes at $PA \sim 40^0$ and 220^0. These lobes are not so prominent in the optical R-band image, nor in the 15 μm ISO image by Cesarsky et al. (1996). The maxima of these lobes match nicely with the maxima of the CO spiral arms but are about $5''$ inside the spiral arms as seen in both R and H α (Garcia-Burillo et al. 1993).

For M 101 the situation is less clear. Fig. 2 shows the central part of the CO map taken from Kenney et al. (1991), observed with an angular resolution of $55''$, comparable to that of the ISO maps. Although the 60 μm emission is less centrally concentrated than the CO (Kenney et

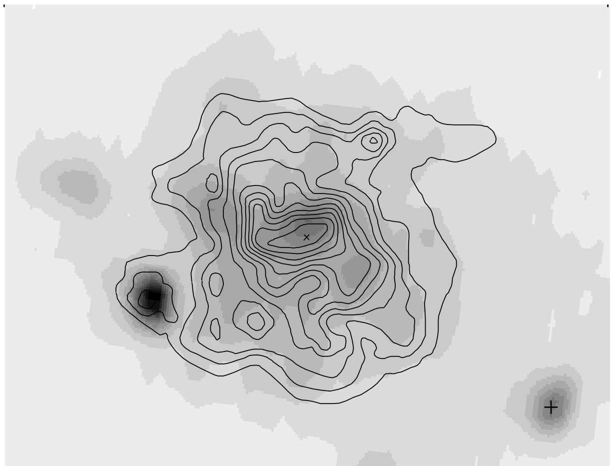

Fig. 2. CO isocontour map for the central $16' \times 12'$area of M 101 (from Kenney et al. 1991), overlaid on the 60 μm map.

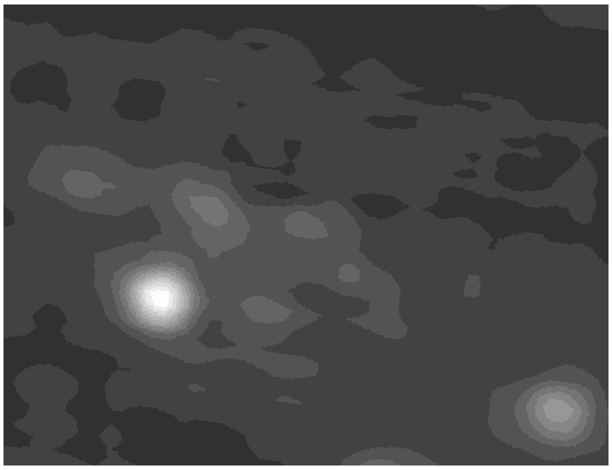

Fig. 3. Color difference map (60 μm-0.21×100μm) for M 101, for the same area as in Fig. 2. The bright spot is the H II region NGC 5461.

al. 1991), the more detailed 60 μm morphology of M 101 otherwise resembles both the the CO and H α distributions, in contrast to the case for M 51. These similarities in M 101 result from this galaxy's later Hubble type (Sc); the angular resolution considered here is insufficient to probe the more complex - compared to the Sbc class - arm system that is a defining property of the Sc class.

In order to compare the ISOPHOT maps at different wavelengths we adjusted their spatial resolutions by using appropiate gaussian convolutions. Thus, the comparison between the 60 μm and 100 μm maps is done at the resolution of the 100 μm map. In Fig. 3 we show the difference map $S(60) - 0.21 \times S(100)$, with the factor 0.21 according to the value for the average cirrus background (Désert et al. 1990). Except for the bright H II regions the disk disappears almost completely in this difference map, which not only means that the intensity ratio and thus the temperature are rather constant over the whole disk, but also that the diameter of the galactic disk at 60 μm is, within the accuracy of the data, identical with that at 100 μm (we therefore do not show radial intensity profiles).

In the case of M 51 the difference map is not so flat since the spatial resolution is too low at 100 μm to properly discriminate the double lobe structure. A bright residuum is seen at NGC 5195 where the S(60)/S(100) ratio is considerably higher, as previously noted (Telesco et al, 1988).

For quantitaive color information, we summarise in Table 1 the integrated fluxes for selected fields in M 101 of size $75'' \times 75''$. Column 2 gives a description or the names for the H II regions, columns 3 and 4 the offsets from the galaxy center, columns 5–7 the flux densities at 60, 100, and 175 μm. For the 60 μm data the map was smoothed to the same angular resolution as the 100 μm map. Column 8 gives the temperature for the fitted blackbody curve multiplied by the emission efficiency (see Fig. 4). Columns 9 & 10 give the integrated fluxes, as described at the end of this section. For a few of the regions in M 101 FIR flux densities are also given in the IRAS point source catalog; they are mostly somewhat higher than the ISOPHOT values due to the larger aperture used.

In order to see the influence of the star forming regions on the FIR emission, the available Hα fluxes for the H II regions (Israel & Kennicutt 1980) are given in Column 11. Devereux & Scowen (1994) have reported good correspondence of the FIR values with Hα fluxes. Comparing the data in our table we, however, see little correlation, even when taking into account the visual absorption (Israel & Kennicutt). This is especially true for NGC 5471, which is the brightest H II region but almost an order of magnitude fainter in the FIR than NGC 5461. The last column gives the available 60 μm IRAS fluxes.

Figure 4 displays the spectral energy distributions for characteristic fields in M 101. The 60 and 100 μm values are taken from the table, and the 175 μm values are adapted to the other two data points, by scaling them with the inverse of the factor by which the 100 μm fluxes change when they are smoothed to the angular resolution of the 175 μm map. Assuming the emission efficiency to vary as λ^{-1}, the curves fit well in all cases within the accuracy of our data. This plot indicates that there is no 'undiscovered' cold dust ($\sim$ 15 K) component as seen for interacting galaxies (Klaas et al. 1996) and that single-temperature emission can fit the observed intensities.

The maximum of the fit curves in Fig. 4 is always situated between 100 μm and 175 μm. Thus, the additional 175 μm data allows an accurate determination of the total FIR luminosity of the galaxies, which for IRAS was only approximately possible (Lonsdale et al. (1981). Unexpectedly, in M 101 there is no systematic difference between arm and interarm regions and no evidence for a radial gradient of color temperature. This indicates that FIR colors are insensitive to the intensity of the interstellar radiation

Table 1. FIR properties for selected fields in M 51 and M 101.

Description		Offset from center		S(60)	S(100)	S(175)	Temp	FIR	F(Hα)	IRAS(60)
		$\Delta\alpha$	$\Delta\delta$	Jy	Jy	Jy	K	10^{-13}Wm^{-2}	10^{-15}Wm^{-2}	Jy
M 51	center	0′.0	0′.0	22.2	85.0	43.9	30.7	15.7		32.0
	SW lobe	-1′.2	-1′.5	9.6	34.6	24.1	33.3	7.6		
	NE lobe	1′.1	1′.5	11.8	43.3	25.4	30.0	8.4		
	companion	1′.0	4′.3	7.7	19.4	8.9	31.7	4.1		10.0
M 101	center	0′.0	0′.0	5.0	20.5	14.2	28.8	4.2		3.9
	NGC 5461	4′.0	-1′.8	6.0	14.0	7.1	32.9	3.2	3.2	9.6
	NGC 5447	-6′.7	-4′.7	3.3	8.0	4.3	32.1	1.8	1.6	4.9
	NGC 5449	-5′.5	-1′.1	1.1	4.2	3.2	29.2	0.9	0.5	
	NGC 5455	-1′.8	-6′.5	1.6	3.6	3.4	29.5	1.0	1.8	1.6
	Hodge 40	2′.5	0′.2	4.0	15.0	11.5	29.0	3.0	0.8	
	NGC 5462	5′.9	1′.1	1.9	5.6	3.2	31.5	1.2	1.5	
	NGC 5471	11′.1	3′.0	1.3	2.3	1.5	31.4	0.5	3.6	1.8
	inner arm	-0′.2	-2′.6	2.8	12.1	11.3	27.9	2.5		
	south. arm	2′.4	-3′.5	1.7	6.5	7.0	27.4	1.5		
	interarm SW	-2′.2	-4′.1	1.3	5.3	5.8	27.4	1.2		
	interarm E	4′.3	0′.5	1.5	4.2	4.7	29.1	1.0		

field. A similar result was found from IRAS observations for the S(60)/S(100) ratio (Rice et al. 1990).

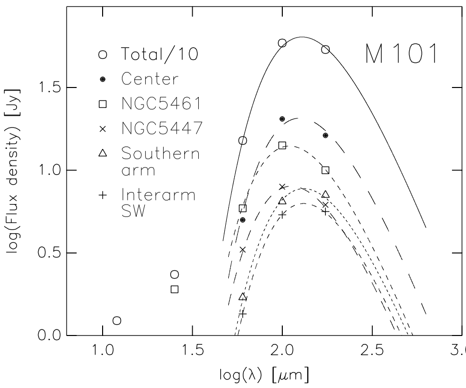

Fig. 4. Spectral energy distributions F_ν for M 101.

3. Preliminary Conclusions.

The far-IR maps of M 51 and M 101 show bright nuclei and extended emission that is generally correlated with the CO distributions, but also with the distributions of star formation. Assuming an emissivity that varies with λ^{-1}, the dust temperatures across M 51 and M 101 are in the range 28–33 K. Unlike the warm dust, which dominates the emission at 15 μm and traces the regions of recent star formation, the far-IR-emitting dust shows no obvious correlation in temperature with the star forming regions.

The reason for this seems to be that we see two different populations of dust. Small dust grains in the star forming regions are heated by the UV radiation and most evident at 15 μm. The cooler dust, consisting of large grains, is mainly heated by the softer, more diffuse, interstellar field and and also probably better traces the dust mass distribution and the mass distribution of the molecular gas (Walterbos & Greenawalt 1996). This picture is only a first approximation, since very small, transiently heated grains cause the temperature of the general interstellar medium to be hotter than the equilibrium values (see, e.g., Telesco 1993).

Acknowledgements. This letter is based on observations with ISO, a project of ESA with the participation of ISAS and NASA. The ISOPHOT project was funded by the Deutsche Agentur für Raumfahrtangelegenheiten (Bonn) and by the Max-Planck Gesellschaft.

References

Cesarsky, C. et al. 1996, (*this volume*)
Désert, F.-X., Boulanger, F., Puget, J.L. 1990, A&A 237, 215
Devereux, N.A., Scowen, P.A. 1994, AJ 108, 1244
Garcia-Burillo, S., Guélin, M., Cernicharo, J. 1993, A&A 274, 123
Hippelein, H. et al. 1996, (Letter I, *this volume*)
Israel, F.R., Kennicutt, R.C. 1980, Ap.Lett. 21, 1
Kenney, J.D.P., Scoville, N., Wilson, C. 1991, ApJ 366, 432
Klaas, U., et al. 1996, (*this volume*)
Lonsdale et al. 1981, *IRAS Extragalactic Catalog*
Rice, W. et al. 1988, A&ASS 68, 91
Rice, W. et al. 1990, ApJ 358, 418
Telesco, C.M. Wolstencroft, R., Done, C. 1988, ApJ 329, 174
Telesco, C.M. 1993, in *Infrared Astronomy*, eds. A. Mampaso et al., Cambridge Univ. Press, p.173
Walterbos, R.A.M., Greenawalt, B. 1996, ApJ 460, 696